

Variable interhemispheric asymmetry in layer V of the supplementary motor area following cervical hemisection in adult macaque monkeys

<https://doi.org/10.1523/ENEURO.0280-20.2020>

Cite as: eNeuro 2020; 10.1523/ENEURO.0280-20.2020

Received: 29 June 2020

Revised: 24 August 2020

Accepted: 3 September 2020

This Early Release article has been peer-reviewed and accepted, but has not been through the composition and copyediting processes. The final version may differ slightly in style or formatting and will contain links to any extended data.

Alerts: Sign up at www.eneuro.org/alerts to receive customized email alerts when the fully formatted version of this article is published.

Copyright © 2020 Contestabile et al.

This is an open-access article distributed under the terms of the Creative Commons Attribution 4.0 International license, which permits unrestricted use, distribution and reproduction in any medium provided that the original work is properly attributed.

Variable interhemispheric asymmetry in layer V of the supplementary motor area following cervical hemisection in adult macaque monkeys.

A. Contestabile^{1,2}, R. Colangiulo², M. Lucchini^{1,2}, E. M. Rouiller² and E. Schmidlin²

⁽¹⁾ Department of Basic Neuroscience, University of Geneva; 1, Rue Michel-Servet, CH-1205 Genève, Switzerland.

⁽²⁾ Department of Neurosciences and Movement Sciences, Section of Medicine, Faculty of Sciences and Medicine, Fribourg Center of Cognition, University of Fribourg, Chemin du Musée 5, CH-1700 Fribourg, Switzerland.

Running title: SMA asymmetry in SCI monkeys

Keywords: spinal cord injury, supplementary motor area, layer V pyramidal neurons, corticospinal projections, interhemispheric asymmetry, SMI-32, non-human primate.

Text pages: 28

Words: 6364 total words (without abstract, significance statements, acknowledgments, list of references and figure legends). Abstract: 146 words. Introduction: 981 words. Material and Methods: 2021 words. Results: 1506 words. Discussion: 1856 words. Tables: 1. Figures: 5.

Post-revision corrections after revision in *eNeuro* are labelled in red.

Address for correspondence: Dr. Eric Schmidlin, Department of Neurosciences, Faculty of Sciences and Medicine, University of Fribourg, Chemin du Musée 5, CH-1700 Fribourg,

27 Switzerland. Phone: +41 26 300 86 09. Fax: +41 26 300 96 75. E-mail:

28 Eric.Schmidlin@unifr.ch

ABSTRACT

Motor cortical areas from both hemispheres play a role during functional recovery after a unilateral spinal cord injury (SCI). However, little is known about the morphological and phenotypical differences that a SCI could trigger in corticospinal neurons of the ipsilesional and contralesional hemisphere. Using an SMI-32 antibody which specifically labeled pyramidal neurons in cortical layers V, we investigated the impact of a unilateral cervical cord lesion on the rostral part (F6) and caudal part (F3) of the supplementary motor area (SMA) in both hemispheres of eight adult macaque monkeys compared with four intact control monkeys. We observed in F3 (but not in F6) interindividual variable and adaptive interhemispheric asymmetries of SMI-32 positive layer V neuronal density and dendritic arborization, which are strongly correlated with the extent of the SCI as well as the duration of functional recovery, but not with the extent (percentage) of functional recovery.

Significance statement

1. This study consists in a precise quantification on two different levels of the histological consequences on the long term of a traumatic and sudden unilateral interruption of the corticospinal tract at cervical level in 8 non-human primates (adult macaque monkeys).
2. The lesion affected the density and the morphology of layer v pyramidal neurons in the supplementary motor area (SMA), in the form of an interhemispheric adaptive asymmetry, correlated to the lesion size and duration of functional recovery.
3. These changes are reminiscent of those observed in SMA after unilateral lesion of the primary motor cortex, suggesting to some extent comparable mechanism of functional motor recovery from unilateral cortical or spinal lesion.
4. The dendritic arborization in the basal dendrites of the SMI-32 positive neurons in layer V showed a more prominent interhemispheric effect of the lesion than the apical dendrites.

Introduction

In non-human primates, the hand area of the primary motor cortex (M1 or F1) is subdivided in an old M1 and a new M1 (Rathelot and Strick, 2009). The new M1 is at the origin of the corticomotoneuronal (CM) projection, representing the anatomical support of manual dexterity, a prerogative of primates (Lawrence and Kuypers, 1968; Courtine *et al.*, 2007; Lemon, 2008; Yoshida and Isa, 2018). Although M1 is the main contributor to the corticospinal (CS) projection (including the CM projection), non-primary motor areas such as the premotor cortex (PM), the supplementary motor area (SMA-proper or F3) and the cingulate motor areas (CMA) are also at the origin of CS projections (Luppino *et al.*, 1994; Rouiller *et al.*, 1994; Dum and Strick, 1996; Rouiller, 1996). In particular, SMA projects to the cervical spinal cord, where the motoneurons controlling hand (fingers) motor function are located (Jenny, Inukai and Strick, 1983). There is evidence that part of the CS projection from SMA may be CM (Rouiller, 1996), but the influence of SMA on hand motoneurons is functionally less strong than the one of M1 (Maier *et al.*, 2002; Boudrias *et al.*, 2010). The multiple representations of the hand in several motor cortical areas (M1, PM, SMA, CMA) of primates is the basis for a vicarious scenario of functional redistribution of hand function control in case of selective and focal lesion affecting a motor structure. For instance, after unilateral lesion of the hand area in M1 functional recovery, though often incomplete, depends on plasticity of intact non-primary motor areas, such as PM (Liu and Rouiller, 1999; Dancause *et al.*, 2005; Hoogewoud *et al.*, 2013; Orczykowski *et al.*, 2018) and/or SMA (McNeal *et al.*, 2010; Morecraft *et al.*, 2015). Although such rearrangement of the cortical motor circuits is believed to occur mostly in the ipsilesional hemisphere, there is still controversy about the role played by the contralesional hemisphere (see e.g. (Morecraft *et al.*, 2016; Savidan *et al.*, 2017) for the non-human primate). In a recent article from this laboratory, we reported that a unilateral lesion of the M1 hand area led to a variable interhemispheric asymmetry in the detection of layer V pyramidal neurons in SMA, identified with the marker SMI-32 (Contestabile *et al.*, 2018). This anatomical variable interhemispheric

imbalance possibly reflects an adaptive interhemispheric contribution of the bilateral SMA to recovery, depending on the lesion size as well as on the duration of functional recovery (Contestabile *et al.*, 2018). It was argued that these observations may represent a putative anatomical support of diaschisis, originally defined as a “*loss of function and electrical activity in an area of the brain due to a lesion in a remote area that is neuronally connected with it*” (Finger, Koehler and Jagella, 2004 and see von Monakow, 1914). In other words, due to a unilateral M1 lesion, the function of the SMA is affected at distance differently on the ipsilesional versus contralesional hemispheres, because the reciprocal connections between M1 and SMA are stronger ipsilaterally than contralaterally, in the intact state. More recently, the concept of diaschisis has been extended to a structural dimension, in the form of “connectional diaschisis”, focused on post-lesion changes of connectivity in networks/circuits directly or indirectly related to the focal lesion site (Carrera and Tononi, 2014).

In the current study, the main goal was to transpose this concept of interhemispheric adaptable SMA reorganization related to functional recovery from a lesion of M1 (Contestabile *et al.*, 2018) to a cervical spinal cord hemisection. Does a unilateral spinal cord injury (SCI) also affect differently the contralesional versus the ipsilesional SMA, because the CS projection from SMA is predominantly crossed (**Fig. 1A** and **B**)? Following a hemisection of the cervical cord in macaque monkeys, it was observed that the CS axotomy did not lead to a retrograde death of CS neurons in M1 (Wannier *et al.*, 2005), but instead to a somatic shrinkage of CS neurons in layer V of the contralesional M1 (Beaud *et al.*, 2008). As far as the functional recovery from CS tract injury or cervical cord lesion is concerned, the underlying mechanisms are multiple and complex, involving plasticity at spinal, subcortical and cortical levels, depending also on the time course of rehabilitative training (Galea and Darian-Smith, 1997; Freund *et al.*, 2007; Nishimura *et al.*, 2007; Nishimura and Isa, 2009, 2012; Zaaïmi *et al.*, 2012; Sugiyama *et al.*, 2013; Isa and Nishimura, 2014; Chao *et al.*, 2019). At cortical level in particular, following unilateral cervical lesion, the bilateral M1 areas are involved in the functional recovery at early stage whereas, at later stage, the contralesional M1 area plays a major role, together with the bilateral PM (Freund *et al.*, 2007;

111 Nishimura *et al.*, 2007; Nishimura and Isa, 2012; Isa and Nishimura, 2014). Moreover, a
112 recent study identified two distinct cortical network dynamics that are implicated in the
113 recovery of a unilateral SCI: the grasping-related intrahemispheric interactions from the
114 contralesional PM to the contralesional M1, and motor-preparation-related interhemispheric
115 interactions from the contralesional to ipsilesional PM (Chao *et al.*, 2019).

116 What happens in SMA layer V bilaterally after cervical hemisection and functional
117 recovery? One may hypothesize that CS neurons in SMA also survive (as those in M1: see
118 above), but their phenotype is likely to be modified (connectional diaschisis), in a variable
119 manner depending on the hemisphere (because of the asymmetric strength of its CS
120 projection), as well as on lesion parameters, such as lesion extent, as well as on functional
121 recovery parameters (duration of recovery, extent of recovery,). To test these different
122 hypotheses, SMI-32 labelled neurons in the bilateral SMAs were analyzed histologically in
123 eight macaque monkeys subjected to cervical hemisection and compared to intact monkeys
124 (n = 4), based on the assumption that graded changes in the phenotype of CS neurons in
125 SMA impacts on the detection of those neurons using the marker SMI-32 (see (Contestabile
126 *et al.*, 2018); see also (Geyer *et al.*, 2000)).

Material and methods

The methods to analyze the histological sections in SMA following SCI were similar to those reported in detail in a recently published open access article (Contestabile *et al.*, 2018), also focused on SMA but following a lesion of the primary motor cortex (M1). Nevertheless, for the sake of convenience, the methods are reminded here, though in a somewhat shorter version.

Macaque monkeys

The present histological analysis in SMA was conducted on 12 adult macaque monkeys (10 *Macaca fascicularis*, 2 *Macaca mulatta*; Table 1). All procedures were conducted in accordance with guidelines of the federal and local (cantonal) veterinary authorities (veterinary authorizations: 157e/04, 175/04, 187/05, 188/06, 193/07). All 12 monkeys included in the current study were already reported in previous articles addressing distinct issues related to C7 spinal cord lesion (Freund *et al.*, 2006, 2007, 2009; Beaud *et al.*, 2008, 2012; Hoogewoud *et al.*, 2013) or as intact control animals (Contestabile *et al.*, 2018). Eight animals (Mk-CG, Mk-CGa, Mk-CH, Mk-CP, Mk-CS, Mk-AG, Mk-AM and Mk-AP) were subjected to a unilateral cervical cord lesion at C7 level, for whom detailed and comprehensive experimental data were reported previously, such as lesion characteristics, behavior, plasticity of CS projection system in M1 and at spinal cord level, effects of the anti-Nogo-A antibody therapy (Freund *et al.*, 2006, 2007, 2009; Beaud *et al.*, 2008, 2012; Hoogewoud *et al.*, 2013). Four other monkeys (Mk-IC, Mk-IE, Mk-IR, and Mk-IZ) had no lesion (intact monkeys) and were used as controls; they already appeared as such in a recent study (Contestabile *et al.*, 2018). Three out of eight cervical cord lesioned monkeys were treated with anti-Nogo-A antibody (Mk-AG, Mk-AM and Mk-AP). Comprehensive descriptions of the anti-Nogo-A antibody treatment procedure were published earlier (Freund *et al.*, 2006, 2007, 2009; Beaud *et al.*, 2008, 2012; Hoogewoud *et al.*, 2013). In short, the anti-Nogo-A antibody treatment (14.8 mg) was applied during for 4 weeks immediately after

the SCI. The anti-Nogo-A antibody was delivered from an osmotic pump, placed in the back of the animal. The other five monkeys subjected to SCI received a control antibody (Freund *et al.*, 2006, 2007, 2009). At the end of the behavioral assessments (see below), the animals were euthanized under deep anesthesia obtained with an intraperitoneal overdose of pentobarbital sodium (90 mg/kg body weight), as previously reported (Freund *et al.*, 2006, 2007, 2009; Beaud *et al.*, 2008, 2012; Hoogewoud *et al.*, 2013).

Table 1. Summary of the individual properties of each monkey

	Intact				Untreated				Treated with anti-Nogo-A antibody			
	Mk-IC	Mk-IE	Mk-IR	Mk-IZ	Mk-CG	Mk-CGa ³	Mk-CH	Mk-CP	Mk-CS	Mk-AG ³	Mk-AM	Mk-AP
General information												
Birthday	17.07.99	15.06.96	02.02.04	12.05.96	20.02.01	21.05.03	20.02.01	22.12.97	30.04.97	28.03.02	20.02.01	09.03.98
Sex	M	M	F	M	M	M	M	F	M	M	M	F
Species	Fasc	mul	Fasc	Fasc	fasc	fasc	fasc	fasc	mul	fasc	fasc	fasc
Date of sacrifice	17.08.09	15.02.02	22.12.09	09.02.04	13.01.05	19.01.07	07.02.05	09.11.04	21.09.01	03.08.05	14.02.05	16.11.04
Lesion												
Date of lesion	-	-	-	-	25.08.04	16.08.06	29.09.04	04.05.04	07.03.01	13.04.05	29.09.04	02.06.04
SCI side	-	-	-	-	left	right	right	left	left	left	right	left
Weight at time of lesion (kg)	-	-	-	-	5.1	-	4.1	3.8	4.0	3.7	4.5	4.2
Age at the time of the lesion (days)	-	-	-	-	1282	1183	1317	2325	1407	1112	1317	2277
Hemisection extent (%)	-	-	-	-	51	73	90	45	63	78	80	58
Degree of functional recovery from SCI, total score (%) ¹	-	-	-	-	90	100	53	83	22	100	96	99
Duration of functional recovery (days) ²	-	-	-	-	49	43	41	49	47	7	27	36
Treatment												
Type of antibody	-	-	-	-	ctrl	ctrl	ctrl	ctrl	ctrl	ATI	ATI	11c7
Cocentration (mg/ml)	-	-	-	-	9	7	9	3.7	3.7	3.6	9	3.7
Volume (ml)	-	-	-	-	4	2	4	4	4	2	4	4
Days of antibody injection	-	-	-	-	30	29	28	29	32	28	28	15

M = Male; F = female; fasc = *M. fascicularis*, mul = *M. mulatta* and rhe = *Rhesus*.

¹ Expressed in percentages of postlesion total score at plateau divided by pre-lesion total score in the modified Brinkman board task: all slots.

² Time interval from the day of lesion to the beginning of postlesion plateau, as defined by Kaeser et al. 2011 (Kaeser *et al.*, 2011).

³ Mk-CGa and Mk-AG suffered from a more caudal lesion than C7/C8. These monkeys were taken into account in this study but with some reserves.

160

161 Behavior

As recently reported (Contestabile *et al.*, 2018), manual dexterity was quantified in the eight monkeys subjected to unilateral SCI, based on the “modified Brinkman board” task, testing the precision grip (opposition of thumb and index finger), needed to grasp small food pellets in 25 vertically oriented slots and 25 horizontally oriented slots, randomly positioned over a Perspex board (Schmidlin *et al.*, 2011). After habituation to the housing facility and transfer to a primate chair using positive reinforcement (see <http://www.unifr.ch/neuro/rouiller/home/nhp>), the macaques monkeys were progressively

trained daily to perform the “modified Brinkman board” task, separately for each hand, until they reached a pre-lesion plateau of performance. The duration of the training period and the plateau level of performance was variable across monkeys, as reported earlier based on a large cohort of animals (Kaesler *et al.*, 2014). Then, at plateau, the monkeys were tested daily, once for each hand, during a pre-lesion phase of several weeks in order to establish a score of manual dexterity of reference in the intact monkey. The same behavioral test procedure was pursued also daily after the SCI, without additional training besides the test itself. Based on the post-lesion tests, it was possible to assess the progressive functional recovery from the SCI and the performance level of the post-lesion plateau.

The dramatic drop of score (usually to zero) immediately after the lesion and the deficits of precision grip following such cervical lesion have been reported in detail earlier (Freund *et al.*, 2006, 2007, 2009; Hoogewoud *et al.*, 2013) and are summarized in Figure 1D. After unilateral C7 injury, a progressive though incomplete functional recovery was observed until reaching a plateau of motor performance a few weeks after the SCI (Freund *et al.*, 2006, 2007, 2009; Hoogewoud *et al.*, 2013) (**Fig. 1D**). The behavioral parameter of interest here was the percentage of functional recovery for the ipsilesional hand, given by the average total score (number of pellets retrieved from both vertical and horizontal wells in 30 s) at post-lesion plateau divided by the average total score at pre-lesion plateau (Freund *et al.*, 2006, 2007, 2009; Hoogewoud *et al.*, 2013) (**Fig. 1D**). Moreover, the plots of manual dexterity scores as a function of time were used to define the time duration until the post-lesion plateau was reached (duration of functional recovery) (**Fig. 1D**).

Unilateral cervical cord lesion

The surgical procedure to perform the unilateral lesion was described in detail in previous reports (Freund *et al.*, 2006, 2007, 2009; Beaud *et al.*, 2008, 2012; Hoogewoud *et al.*, 2013), an experimental procedure summarized below. Anesthesia was induced by an intramuscular injection of ketamine (Ketalar; Parke-Davis; 5 mg/kg, i.m.) and atropine was injected i.m. (0.05 mg/kg) to reduce bronchial secretions. Before surgery, the analgesic

Carprofen was delivered (Rymadil, 4 mg/kg, s.c.). Then, deep and stable anesthesia was obtained via a continuous perfusion (0.1 ml/minute/kg) through an intravenous catheter placed in the femoral vein of a mixture of 1% propofol (Fresenius) and a 4% glucose solution. The monkey was positioned in a stereotaxic headholder in a ventral decubitus position, allowing the spinal processes from C2 to Th1 to be exposed, preceding a complete C6 laminectomy and an upper C7 hemi-laminectomy. The dorsal root entry zone at the C7/C8 border was then identified, providing a medial landmark for placing a surgical blade (No. 11; Paragon), which was inserted vertically 4 mm in depth to generate an incomplete section of the cervical cord at C7 level. In most cases, such a section completely interrupted the CS tract in the dorsolateral funiculus unilaterally. Following the SCI, the monkey was kept alone in a separate cage for a couple of days in order to monitor its health condition and provide specific post-operative care (antibiotics, analgesics,).

Histology and neuroanatomical material for analysis

The general histological and analysis methods are similar to those recently reported (Contestabile *et al.*, 2018) and repeated in a shorter version below. After euthanasia, the spinal cord segment (C3-T4) comprising the SCI was cut parasagittally in either three or five series of respectively 50 or 30 μm sections and processed to visualize either BDA, Nissl or SMI- 32 staining (**Fig. 1A-C**). The extent of the cervical cord lesion was measured in consecutive longitudinal sections (scar tissue and absence of neuronal staining) and transposed in a transversal reconstruction to assess the percentage of lesion with respect to the entire corresponding hemi-cervical cord (white and grey matter).

In all monkeys (SCI and intact), the brain was cut in the frontal plane into 50 μm -thick frozen sections with both hemispheres facing each other on the same slide (**Fig. 2A**). Sections were collected in 5 or 8 consecutive series, one of them immunoreacted to visualize the marker SMI-32 (Sternberger and Sternberger, 1983), as previously reported (Liu *et al.*, 2002; Wannier *et al.*, 2005; Beaud *et al.*, 2008). Frontal brain sections were examined under bright-field illumination (at a total magnification of 200x). Brain regions of interest (mostly

SMA) were vectorised using Neurolucida 9 (MBF Bioscience) with a computer-interfaced Olympus BX40 microscope (Olympus Schweiz AG), a computer-controlled motorized stage (Märzhäuser Wetzlar GmbH, type EK 32 75 50) and a digital camera (Olympus U-PMTVC). The Photomicrographs captured with a digital camera were processed using the CorelDraw software (color, brightness, and contrast were not modified) and then quantification was conducted using the software Neuroexplorer (MBF Bioscience) (example in **Fig. 2B-D**). At that step, the investigator of the histological material was blinded against information on animal group (intact versus SCI) and side of the cervical cord hemisection. The size of the SCI expressed as a percentage of hemisection extent were reported previously (Freund *et al.*, 2006, 2007, 2009; Beaud *et al.*, 2008, 2012; Hoogewoud *et al.*, 2013) and are reminded in Table 1. SMA and its two subdivisions (F3 and F6, respectively corresponding to SMA-proper and pre-SMA) in both hemispheres was delineated from M1 or PM laterally and from cingulate motor area (CMA) ventrally, based on cytoarchitectural landmarks (Liu *et al.*, 2002). SMI-32-positive neurons were counted in SMA layers V and the surface of the delineated F3 or F6 was calculated in relation with the defined limits. Based on an exhaustive plotting method (Fregosi and Rouiller, 2017; Fregosi *et al.*, 2017, 2018), the cellular density in layer V of F3, respectively F6, was computed on individual sections. It is the number of identified SMI-32-positive cells in that layer in one hemisphere divided by the corresponding volume of SMA (given by the thickness of the section multiplied by the area-of-interest). The criteria used to include a neuron were the same proposed in our previous article (Contestabile *et al.*, 2018): (1) *SMI-32-positive*; (2) *the soma, the nucleus or the nucleolus and at least four proximal dendrites of the neuron have to be identifiable*; and (3) *the neuron is located in the cortical layer V*. The criteria to set the rostrocaudal limit between F3 and F6, as well as the precise territories of F3 and F6 analyzed were the same as in Contestabile et al. 2018.

Interhemispheric difference of cell density (IDCD)

An interhemispheric difference of cell density (IDCD) in SMA layer V was computed in each histological section by subtracting the SMI-32-positive neuron density in the ipsilesional

SMA (relatively intact side) from the SMI-32-positive neuron density in the contralesional SMA (strongly connected with the SCI) (**Fig. 3 B and D**). Positive IDCD means that more SMI-32 neurons were found in SMA strongly connected to the side where the spinal cord injury was performed, whereas negative IDCD corresponds to a larger number of SMI-32 neurons in layer V of SMA homolateral to the SCI. In intact monkeys, IDCD was expected to be close to zero whereas, in monkeys subjected to SCI, the IDCD was hypothesized to diverge from zero (see **Fig. 5A**, e.g. gray line). As for our previous work (Contestabile *et al.*, 2018), the interhemispheric comparison was made on each individual section, so that the mirrored SMA territories analyzed on each side had comparable area and position.

Single SMI-32 labelled neuron analysis

To investigate whether the unilateral SCI impacted on the microstructure of single SMI-32 positive neurons in SMA layer V, in particular on their dendritic trees, a so-called Sholl analysis for performed, identical to the one reported recently (Contestabile *et al.*, 2018). The sampling and inclusion criteria were similar: *three SMI-32- positive pyramidal neurons of layer V per hemisphere per section were analyzed in four different sections (12 neurons per hemisphere in total) in each of five representative monkeys: two intact monkeys and three monkeys with SCI. The following criteria were applied to specifically select SMI-32-positive neurons: (1) to be representative of the entire region-of-interest, one neuron was picked in each of the dorsal, middle, and ventral parts of the medial wall in F3; and (2) at least intact primary and secondary dendrites and an apical dendrite reaching the layer III without interruption had to be clearly identified.* Two distinct regions of the dendritic tree of each SMI-32 positive neurons were analyzed: the basal dendrites excluding the axon and the apical dendrite.

Statistics

Statistical analysis was conducted with GraphPad Prism 7 (San Diego, CA, USA). The normality of sample distributions was assessed with the Shapiro–Wilk criterion. In each

281 monkey, the statistical significance of IDCs of SMI-32-positive neurons between the
282 ipsilesional and contralesional hemispheres was assessed using a paired t-test or a
283 Wilcoxon test (according to the data distribution) as the neuronal density was directly
284 compared across the two hemispheres on the same section. In order to compare the
285 interhemispheric morphological data and the results of the Sholl analysis, a two-way RM
286 ANOVA with Bonferroni's posttest correction were used (*: p 0.05, **: p 0.01, ***: p 0.001,
287 ****: p 0.0001). Data are represented as the mean \pm s.e.m. and the significance was set at
288 95% of confidence.

Results

Based on a previously available case ((Rouiller, 1996); intact monkey 93-81), subjected to a unilateral injection of the anterograde tracer BDA in the SMA (F3, focused to the hand area), the bilateral distribution of CS axons was established at cervical level. The majority of CS projection originating from SMA crossed the midline (79.7%) whereas only 20.3% of the BDA positive CS axons were located on the ipsilateral side of the cervical cord (11.7% in the dorsolateral part and 8.6% in the ventromedial part) (**Fig. 1A** and **B**). These results suggest that a unilateral cervical cord injury (SCI, **Fig. 1C**) retrogradely impacts more on the contralesional SMA than on the ipsilesional one (connectional diaschisis).

As previously reported (Freund *et al.*, 2006, 2007, 2009; Beaud *et al.*, 2008, 2012; Hoogewoud *et al.*, 2013), eight macaques monkeys (see Table 1) were unilaterally injured at C7 level (SCI animals: Mk-CG, Mk-CGa, Mk-CH, Mk-CP and Mk-CS; SCI + Anti-Nogo-A animals: Mk-AG, Mk-AM and Mk-AP) and the manual dexterity was quantified using the “modified Brinkman board” task. After unilateral C7 injury, the ipsilesional manual dexterity was severely affected, followed by a progressive though incomplete functional recovery, reaching a plateau of motor performance a few weeks after the SCI (**Fig. 1D**). Thanks to this longitudinal quantification of the manual dexterity, it was possible to calculate the extent of functional recovery (in %) of the ipsilesional hand and the time duration needed to reach the post-lesional plateau (duration of functional recovery) (see Table 1 and **Fig. 1D**).

Neuronal density in the layer V of SMA after a SCI

In order to quantify the effect of a unilateral SCI (**Fig. 1C**) on SMA layer V pyramidal neurons, SMI-32 labelled neurons in the bilateral F3 (SMA-proper) and F6 (pre-SMA) were analyzed histologically in eight macaque monkeys subjected to cervical hemi-section and compared to intact monkeys (n = 4). First, we quantified the density of SMI-32 positive layer V neurons in the delimited F3 and F6 areas in both hemispheres along the rostro-caudal axis in coronal sections (**Fig. 2A–D**). In F6 and F3 layer V, the SMI-32 positive neurons' densities

ranged approximately from 50 cells/mm³ to 250 cells/mm³ across sections/hemispheres/monkeys in the intact group, whereas in the lesioned monkeys, SMI-32-positive neurons' densities in SMA layer V ranged approximately from 100 to 700 cells/mm³ (**Fig. 2E**). With respect to those ranges of cellular densities, in the SCI group, there is no obvious difference between the anti-Nogo-A antibody treated monkeys (n = 3) and the control antibody treated animals (n = 5). In addition, the range of SMI-32-positive neurons' densities in the SMA of SCI animals seemed to reach higher values than the intact group (in fact higher than 3 intact monkeys with low cellular densities in F3, whereas the fourth intact monkey exhibits a cellular density comparable to 5 monkeys of the SCI group). However, the very large interindividual variability of the histological staining quality precludes interindividual comparison between the 2 groups of monkeys and strongly affects the absolute quantification of neuronal density. The quality of SMI-32 staining in 3 of the 4 intact monkeys may have been different than in the SCI monkeys, leading to the differences in the absolute numbers of SMI-32 positive neurons between the two groups. On the other hand, the quality of staining does not interfere when the comparison is intraindividual and furthermore restricted to a single histological section. For this reason, we performed a direct comparison between the hemispheres (left hemisphere compared to the corresponding right hemisphere on the same section).

Interhemispheric difference of cell density (IDCD)

As expected, intact monkeys presented no significant difference in their IDCDs for the SMI-32 positive neurons in layer V of F3 (**Fig. 3A-B**). On the other hand, the IDCDs of SMI-32 positive neurons were significantly different in six out of eight monkeys subjected to SCI (**Fig. 3B**). However, the IDCD was not systematically biased toward the same hemisphere (ipsilesional versus contralesional; **Fig. 3B**). Four lesioned monkeys (Mk-CG, Mk-CGa, Mk-CP and Mk-AP) exhibited a significantly higher contralesional density of SMI-32 positive neurons in F3 layer V, corresponding to a positive IDCD, while two SCI monkeys (Mk-AG

and Mk-AM) had a significantly higher ipsilesional density of SMI-32 positive neurons in F3 layer V, corresponding to a negative IDCD (**Fig. 3A-B**).

In order to have an internal control, the cellular density of SMI-32 positive neurons was also quantified in the layer V of F6 (pre-SMA), a motor cortical area lacking corticospinal neurons (Luppino *et al.*, 1994). The assessment of cellular density in F6 layer V showed no significant IDCD, both in intact animals and in SCI animals (**Fig. 3C-D**). This observation indicates that SMI-32 positive neurons in F6 layer V were not affected by the SCI, as expected.

Finally, we did not observe significant difference between the calculated IDCD between intact and injured animals neither in F3 nor in F6 (**Fig. 3B' and D'**).

Arborization of layer V SMI-32 positive neurons in F3 after SCI

Microstructural changes of the basal (**Fig. 4A**) and apical dendritic (**Fig. 4G**) arborization of SMI-32 positive neurons located in layer V of F3 was assessed based on a Sholl analysis conducted in two control animals (Mk-IR and Mk-IE) and in three representative lesioned monkeys (Mk-CGa, Mk-CP and Mk-AG). For all five animals, the Sholl analysis yielded a classical inverted U-shape curve with a tail on the right, corresponding to an increase of dendritic intersection numbers going away from the soma up to a peak, followed by a comparable progressive decrease ending with slower fading at larger distances from the soma. In most analyzed monkeys, the number of dendritic intersections peaked at a distance of about 50 μ m from the soma, both for basal and apical dendrites (**Fig. 4**). As expected, no interhemispheric difference was observed in the 2 control monkeys for both the basal (**Fig. 4B-C**) and apical dendrites (**Fig. 4H-I**). After SCI, 2 out of 3 monkeys exhibited in F3 interhemispheric differences in the basal dendritic arborization (**Fig. 4D-F**). In fact, for Mk-CP and Mk-AG we observed the same interhemispheric bias consistent with the IDCD bias already observed for layer V in F3 (**Fig. 3B, 4E-F**) for the basal dendrites. A comparable tendency (not statistically significant) was observed for Mk-CGa, the third representative lesioned animal. This significant interhemispheric difference of basal dendritic

arborizations was verified within a limited distance range from the soma, going from 40 to 80 μm . (**Fig. 4E-F**). Interestingly, and in contrast to the basal dendrites, the apical dendrites exhibited clearly less pronounced interhemispheric difference in their numbers of dendritic intersections (**Fig. 4J-L**).

Relationship of IDCs in F3 with percentage of hemi-section extent, duration and extent of functional recovery after SCI

Are the morphological interhemispheric changes on SMI-32 positive neurons in F3 layer V induced by SCI (Figs. 2-3) related to the characteristics of the lesion (size) and/or the properties of functional recovery? To this aim, IDCs of SMI-32 neurons in F3 were plotted as a function of lesion extent (percentage of hemi-section), durations of functional recovery and extent in percent of functional recovery (**Fig. 5A-C**). Interestingly, IDCs in F3 layer V were significantly inversely correlated with the size of the SCI, expressed as the percentage of hemi-section (**Fig. 5A**; $R = -0.857$, $p = 0.006$), independently of the presence/absence of anti-Nogo-A antibody treatment. A similar inverse correlation was found between IDCs and lesion size in F3 after unilateral M1 lesion (Contestabile *et al.*, 2018). In both cases, these correlation data indicate that a small lesion (ipsilateral in the case of cortical lesion or contralateral in case of SCI) is associated with a largely positive IDC whereas large lesions are associated to negative IDCs.

The relationship between the median IDC values and the duration of functional recovery from SCI (**Fig. 5B**) was then investigated, based on behavioral data derived from the modified Brinkman board task: the IDCs in F3 layer V were correlated with the duration of functional recovery (**Fig. 5B**; $R = 0.734$, $p = 0.038$), again independently of the presence/absence of treatment. Interestingly, there was no statistically significant correlation between the duration of functional recovery from SCI and the hemi-section extent of the spinal cord (**Fig. 5C**; $R = -0.525$, $p = 0.181$). However, the 3 SCI monkeys which received the anti-Nogo-A antibody treatment recovered faster (shorter time to reach the post-lesional plateau) than the control antibody treated monkeys, a difference already visible in panel B of

399 Figure 5. In contrast to the parameters lesion extent and duration of functional recovery,
400 IDCDs in F3 layer V were not correlated with the parameter extent of functional recovery
401 (expressed in %) (**Fig. 5D**; $R = 0.054$, $p = 0.889$), assessed with the total score of pellets
402 retrieval in the modified Brinkman board task. Finally, as observed in Contestabile et al.
403 2018, no correlation was observed between the percentage of functional recovery in the
404 modified Brinkman board task and duration of functional recovery (**Fig. 5E**; $R = 0.176$, $p =$
405 0.301) suggesting that a longer duration of functional recovery did not mean a better
406 functional recovery.

Discussion

The major conclusion of the present study is that a unilateral cervical cord hemi-section retrogradely induced an interhemispheric asymmetry of SMI-32 staining in F3 layer V in non-human primates, which is correlated with the extent of the SCI as well as the duration of functional recovery, but not with the extent (percentage) of the functional recovery. These conclusions are coherent with the observations described recently by our laboratory showing similar results in F3 layer V in SMA after a unilateral M1 lesion (Contestabile *et al.*, 2018). A coherent correlation between IDCs and lesion size as well as duration of functional recovery (but not extent of recovery) were observed in this study. In other words, the interhemispheric effects on SMI-32 staining in F3 layer V observed after M1 lesion (Contestabile *et al.*, 2018) can be generalized to another type of unilateral lesion, namely a cervical cord hemi-section. If the morphological interhemispheric changes reflect variable balanced contributions of the two hemispheres in the process of functional recovery, then comparable mechanisms of functional recovery at cortical level may take place, irrespective of the site of lesion (cortical or spinal), at least for injury restricted to one side of the brain or of the spinal cord.

The lateralization of the unilateral lesion, either in M1 or at cervical cord level, is of importance. The computation formula to establish the IDC was chosen to be reversed in the present study (cervical cord lesion) as compared to our recent report on unilateral M1 lesion (Contestabile *et al.*, 2018). The reason for such reversal is that the unilateral M1 lesion was on the same hemisphere as the F3 area, which exhibits (before the lesion) the quantitatively predominant corticocortical connection with the injured M1, whereas the transcortical connection from the opposite F3 is less strong (see (Contestabile *et al.*, 2018); their Fig. 1). In case of cervical cord hemi-section, the predominant corticospinal projection from F3 is crossed (originating mainly from the opposite hemisphere), reason why the IDC formula was reversed (see methods above). Due to this reversal, then the correlation plots in the M1 lesion model ((Contestabile *et al.*, 2018); their Fig. 5) and in the present study (Fig. 5)

should appear similar, if the same correlations are verified. This is indeed the case for the correlation between IDCDs and the lesion extent (compare Fig. 5B of (Contestabile *et al.*, 2018) and the present Fig. 5A). In contrast, although there is a correlation in both lesion models between IDCDs and duration of functional recovery, the correlation was inverse in the M1 lesion model ((Contestabile *et al.*, 2018); their Fig. 5F) and positive in the present SCI model (Fig. 5B). As argued above, due to the reversal of the IDCD formula, we would have intuitively expected a similar correlation direction. This is not the case, suggesting that the mechanisms of recovery reflected by the correlation between IDCD and duration of functional recovery may be independent of the lateralization of the unilateral lesion, either cortical or cervical.

Connectional diaschisis

The results obtained in Contestabile et al. (2018), and in this study could be linked with the old concept of *diaschisis* (von Monakow, 1914), defined as a “loss of function and electrical activity in an area of the brain because of a lesion in a remote area that is neuronally connected with it”, although it corresponds more to a “connectional diaschisis” (Carrera and Tononi, 2014; see introduction above). The unilateral SCI may have affected the morphology, phenotype and cellular expression of layer V neurons in the contralesional hemisphere in a different manner with respect to the neurons localized in the ipsilesional hemisphere. This interhemispheric difference in phenotype could have influenced the affinity for the SMI-32 antibody and explain the observed interhemispheric asymmetry of density of SMI-32-positive layer V neurons. This interpretation is moreover supported by the neuronal reconstruction. In fact, the directions of interhemispheric differences in dendritic arborization complexity (Fig. 4) were consistent with the direction of the IDCD especially in the arborization of the basal dendrites which are more implicated in the integration of the neuronal response and have a strong effect on action potential output due to their direct attachment to the cell body and the proximity to the axon (Nevian *et al.*, 2007; Zhou *et al.*, 2008). The changes of dendritic arborization following spinal cord injury can be linked to the

recently published observation depicting that axotomy of peripheral motor projections induce changes in the dendritic arborization of M1 pyramidal neurons in the rodent model submitted to a permanent lesion of the facial nerve (Urrego, Troncoso and Múnera, 2015). In another recent study aiming at measuring the structural changes in the CNS of human patients suffering from degenerative pathology affecting interaction between cortical motoneurons and spinal motoneurons such as Amyotrophic Lateral Sclerosis (ALS) or dementia, the authors observed a degeneration of the apical dendrites of pyramidal neurons located in layer V of M1 (Betz's cells as described in the paper), to a larger extent in patients suffering from ALS-(Genç *et al.*, 2017). These results are consistent with a lower dendritic arborisation observed in the contralesional SMA (fig. 4 G, L) in animals having a larger extent of SCI, as ALS is a major degenerative disease affecting a majority of motoneurons in the ventral horn of the spinal cord.

Interestingly, it seems that anti-Nogo-A antibody treatment does not have an effect on the observed interhemispheric difference in phenotype. The three treated animals showed results that are comparable to only lesioned animals. Neutralization of Nogo-A was found to promote sprouting of corticospinal axons in macaque monkeys and to lead to a complete recovery of the manual dexterity after a unilateral hemisection lesion irrespectively on the lesion extent (Freund *et al.*, 2006, 2007, 2009). However, it is possible that anti-Nogo-A antibody treatment could not preserve the phenotype of F3 layer V pyramidal neurons since the SCI immediately affect the neuronal connection and altered the phenotype of the corticospinal neurons in an irreversible manner.

A possible role of the ipsilesional hemisphere during the functional recovery from SCI

The correlation between IDCD asymmetry and the duration of functional recovery is also reminiscent of the controversy related to the respective contributions of the ipsilesional versus contralesional hemispheres in the functional recovery following a unilateral SCI. Previous studies in rodents (Ghosh *et al.*, 2009) and humans (Lundell *et al.*, 2011) demonstrated that the ipsilesional hemisphere underwent a profound reorganization of the

motor areas after cervical SCI. Moreover, these previous findings suggest a correlation between brain activity, duration and extent of functional recovery and are consistent with our results. In fact, they revealed that monkeys with larger lesion tend to show shorter duration of functional recovery and negative IDCD suggesting a more prominent reorganization and a predominant contribution of the ipsilesional hemisphere (as compared to the contralesional one), immediately after severe SCI. On the other hand, the data also show that a more moderate lesion leads to a higher SMI-32 positive neurons density in the contralesional hemisphere suggesting a more important reorganization of the hemisphere predominantly affected by the spinal hemisection. Interestingly, previous studies reported an upregulation of the expression of Sema3A and NRP-1 in motoneurons located in the contralesional hemisphere after SCI in rats (De Winter *et al.*, 2002; Hashimoto *et al.*, 2004). It is likely that neurons whose descending fibres were transected upregulated the production of proteins involved in the regulation of axonal re-growth and maintenance. This phenomenon may possibly be correlated with the higher density of neurons in the contralesional hemisphere that express SMI-32, a major component of the neuronal cytoskeleton providing structural support to the axon. However, in a recent study based on meta-analysis of fMRI data assessing the possible reorganisation of different regions of the cerebral cortex after spinal cord injury in human patients, the authors showed changes in bilateral SMA, but were unable to specify the type of change or potential role in the functional recovery (Wang *et al.*, 2019).

Limitations

The present study involves a limited number of monkeys subjected to SCI (n=8), 5 of them received a control antibody, while 3 monkeys were subjected to anti-Nogo-A antibody treatment, as one may reasonably expect from a non-human primate study, mostly for ethical reasons. However, in spite of the limited number of monkeys, the data are internally coherent (e.g. F3 versus F6) and statistically significant correlations of IDCDs with lesion extent and duration of functional recovery emerged (Fig. 5). Furthermore, these correlation data are fully

consistent with previous data derived from another pool of monkeys (n=9) subjected to another type of unilateral lesion (M1) affecting the CS projection (Contestabile et al., 2018).

An important limitation of this study is due to the impossibility to compare the absolute values of SMI-32-positive neurons' densities across animals. Although the raw data seems to show a higher density of SMI-32 neurons in both hemispheres of SCI monkeys as compared to intact animals, such interindividual comparison between the 2 groups of monkeys is problematic due to a very large interindividual variability of the histological staining quality, strongly affecting the absolute quantification of neuronal density. The quality of SMI-32 staining in 3 of the 4 intact monkeys may have been different (lower) than in the SCI monkeys, leading to the differences in the absolute numbers of SMI-32 positive neurons between the two groups. In one of the intact monkeys (Mk-IC), the absolute cellular density is comparable to that of 5 of the SCI monkeys, corresponding thus to a partial overlap between the 2 groups (which are not statistically different with respect to their IDCDs in F3 and F6 (Fig. **3B** and **D**). On the other hand, the quality of staining does not interfere when the comparison is intraindividual and furthermore restricted to a single histological section (left hemisphere compared to the corresponding right hemisphere on the same section, both hemispheres processed histologically in the very same way and at the same time point).

Further limitations were related to the impossibility in some monkeys to perform the cell counting and consecutive IDCD analysis in F6 because of the lack of brain tissue. Finally, the histological condition of some SMI-32 sections was not optimal to perform the neuronal dendritic reconstruction and for this reason the morphological sholl analysis was limited to 5 animals (**Fig. 4**).

Conclusion

Altogether, the current study on SCI and the recent investigation on M1 lesion (Contestabile et al., 2018) both show that a unilateral lesion affecting the CS projection system, either at its origin (in M1) or along its trajectory (at cervical level) results in a variable and adaptable interhemispheric balance of F3 layer V pyramidal neurons, detected with the marker SMI-32,

545 in a manner which is systematically correlated with the extent of the lesion as well as the
546 duration of the functional recovery of manual dexterity. These observations suggest that the
547 controversy on which hemisphere (ipsilesional versus contralesional) is involved in the
548 functional recovery may be resolved by considering a contribution of both, however in an
549 adaptable and finely tuned balance depending on the lesion properties (e.g. extent) and
550 evolving with time during the recovery, the duration of the latter being a crucial factor in this
551 process.

Acknowledgements

The authors thank the excellent technical assistance of Mrs Véronique Moret, Christine Roulin, and Christiane Marti (histology), of Mr. Laurent Bossy, Joseph Corpataux and Jacques Maillard (animal care taking), André Gaillard (mechanics), Bernard Aebischer and Andrea Francovich (electronics), and Laurent Monney (informatics).

This work was supported by: Swiss National Science Foundation, Grants No 31-61857.00, 310000-110005, 31003A-132465, 310030B-149643 (EMR), No 320030-160229 (ES), the National Centre of Competence in Research (NCCR) on “Neural plasticity and repair”; Novartis Foundation; The Christopher Reeves Foundation (Springfield, NJ, USA); The Swiss Primate Competence Centre for Research (SPCCR:).

Conflict of interest: the anti-Nogo-A antibody was provided by Novartis Pharma AG.

Authors' contribution

A.C. and R.C. performed most of the analysis of the histological data. M.L. and A.C. contributed to the Sholl analysis. A.C., E.M.R. and E.S. prepared the figures and wrote the manuscript. E.M.R. and E.S. coordinated all aspects of the work. E.S. designed and supervised the morphological analysis; EMR designed and coordinated the overall behavioural and lesional study.

Captions to figures

Figure 1- Corticospinal projection of SMA.

(A) Upper panel: schematic representation of a macaque brain showing the location of pre-SMA (area F6), SMA-proper (area F3) and M1. Lower panel: schematic representation of the corticospinal projections of F6 (bilateral). (B) Lower panel: upper cervical spinal cord section showing the localization of CS axons labelled by a unilateral BDA injection in the SMA. Upper panel: Pie chart reporting the percentage of BDA positive CS axons present in the ipsilateral ventromedial, ipsilateral dorsolateral and contralateral dorsomedial part of the spinal cord. The majority of BDA positive CS axons are located in the contralateral dorsolateral part of the spinal cord. (C) Photomicrographs of sagittal histological sections of the spinal cord of a lesioned animal (Mk-CSI) showing the induced permanent lesion at the C7/C8 level. The histological sections derived from two different series processed to visualize SMI-32 staining (left) or Nissl staining (right). Scale bar: 500 μ m. (D) Graphical representation of behavioral performance in the modified Brinkman board task of the macaque monkeys included in this study (SCI in green and SCI + anti-Nogo-A treatment in dark grey). The manual performance of the ipsilesional hand is given by the score (number of pellets retrieved in the first 30 s of the task from the randomly distributed wells) as a function of time (days) before and after a SCI. Day 0 corresponds to the day of the lesion (vertical red line). Pre and post-lesional average of the scores are indicated with horizontal grey lines. The total duration of functional recovery of manual dexterity after lesion is given by the time interval between the lesion (red vertical line) and the onset of the postlesion plateau (brown area). Figure Contributions: EMR and ES performed and supervised the experiments on the monkeys and analyzed the data.

Figure 2 - Neuronal density in the layer V of SMA in intact and SCI monkeys

(A) Photomicrograph of coronal brain histological section of an intact macaque monkey (Mk-IR) stained with SMI-32 and magnified in F3 (scale bar: 40 μ m). Layer III and V are visible and SMI-32 positive pyramidal neurons are indicated with arrows. (B-D). Localization of SMI-

32 positive layer V neurons in bilateral F3 and F6 areas of three representative macaque monkeys (intact: Mk-IR, SCI: Mk-CG and SCI + anti-Nogo-A treatment: Mk-AM). 4 sections per macaque monkeys are shown and the relative rostro-caudal position of the sections from the F3-F6 border is reported in millimeters. Negative distance values belong to F6 and positive distance values belong to F3. **(E)** Graphs representing the rostro-caudal gradient (from F6 to F3) of SMI-32 positive cell density in layer V of all monkeys (intact: Mk-IC, Mk-IE, Mk-IR and Mk-IZ; SCI: Mk-CG, Mk-CGa, Mk-CH, Mk-CP and Mk-CS; SCI + anti-Nogo-A treatment: Mk-AG, Mk-AM and Mk-AP). The cell density for each hemisphere is plotted as a function of the distance from the F3-F6 border, which has been set to 3 mm rostrally to the genu of the arcuate sulcus. Negative distance values belong to F6 and positive distance values belong to F3. The symbol # was used to indicate that the analyzed cortex region was not complete (sections lacking for the analysis). Figure Contributions: EMR and ES performed the experiments on the monkeys and generated the histological sections; AC and RA performed the microscopic analysis of the histological sections; AC analyzed the data.

613

614 **Figure 3 - Interhemispheric difference of cell density (IDCD) after SCI in F3 and F6**

(A) Histograms reporting the cell density of layer V SMI-32 positive neurons in F3 for intact (white background), SCI (light grey background) and SCI treated monkeys (dark grey background). For each couple of histograms, are reported the side (L = left and R = right) and the location in function of the SCI (Ipsi = ipsilesional and Contra = contralesional). As statistical test, a paired t-test or Wilcoxon test was performed (p – values are reported) comparing the cell density in the two hemispheres in each consecutive histological section.

(B) Histograms showing the IDCD of layer V SMI-32 positive neurons of F3 for intact (white background), SCI (light grey background) and SCI treated monkeys (dark grey background). A positive IDCD corresponds to an ipsilesional bias in pyramidal cell density while a negative IDCD corresponds to a contralesional bias in pyramidal cell density. **(B' upper left inset)** Comparison of calculated IDCD in F3 between groups. No statistical difference is observed (unpaired t-test: $t_{(10)} = 0.8276$, $p = 0.4272$). **(C)** Histograms reporting the cell density of layer

V SMI-32 positive neurons in F6 for intact (white background), SCI (light grey background) and SCI treated monkeys (dark grey background). For each couple of histograms, are reported the side (L = left and R = right) and the location in function of the SCI (Ipsi = ipsilesional and Contra = contralesional). As statistical test, a paired t-test or Wilcoxon test was performed (p – values are reported) comparing the cell density in the two hemispheres in each consecutive histological section. **(D)** Histograms showing the IDCD of layer V SMI-32 positive neurons of F6 for intact (white background), SCI (light grey background) and SCI treated monkeys (dark grey background). **(D' upper left inset)** Comparison of calculated IDCD in F6 between groups. No statistical difference is observed (unpaired t-test: $t_{(7)} = 1.084$, $p = 0.3142$). For A and C, the median and the interquartile range are indicated. For B and D, the mean \pm SD are reported. Abbreviations: L = left hemisphere, R = right hemisphere, *: $p \leq 0.05$, **: $p \leq 0.01$). Figure Contributions: EMR and ES performed the experiments on the monkeys and generated the histological sections; AC and RA performed the microscopic analysis of the histological sections; AC analyzed the data.

Figure 4 - Arborization of layer V SMI-32 positive neurons in F3 after a SCI

(A) Neuronal reconstruction example of basal dendrites of a layer V SMI-32 positive neuron. **(B - F)** Sholl profiles of basal dendrites of layer V SMI-32-positive neurons in each hemisphere in two intact monkeys (A-B) and in three SCI monkeys (D-F). For each monkey, the IDCD are reported in the upper right angle. **(G)** Neuronal reconstruction example of apical dendrite of a layer V SMI-32 positive neuron. **(H - L)** Sholl profiles of apical dendrites of layer V SMI-32-positive neurons in each hemisphere in two intact monkeys (H-I) and in three SCI monkeys (J-L). The curves represent the mean intersection values \pm SD. As statistical test, a two-way ANOVA with Bonferroni's multiple comparison post test was performed (*: $p \leq 0.05$, **: $p \leq 0.01$, ***: $p \leq 0.001$). The p - values for the distance to soma main effect (up) and hemisphere main effect (right) are report for each monkey. # in the upper right angle means a significative p – value for the interaction between the distance to

soma and the hemisphere main effect. Figure Contributions: AC and ML performed the microscopic analysis of the histological sections; AC analyzed the data.

Figure 5 - Relationship of IDCD, proportion of hemisection extent, duration of recovery and percentage of functional recovery

(A) The interhemispheric difference in cell density (IDCD) in F3 was plotted in function of the proportion of hemisection extent. The gray line represents the hypothesized interhemispheric cell density asymmetry (see introduction). **(B)** The interhemispheric difference in cell density (IDCD) in F3 was plotted in function of the duration of functional recovery. **(C)** The duration of functional recovery was plotted in function of the proportion of hemisection extent. **(D)** The interhemispheric difference in cell density (IDCD) in F3 was plotted in function of the functional recovery. **(E)** The functional recovery of the animals was plotted in function of the duration of functional recovery. Intact (in white), SCI (light gray) and SCI treated (dark gray) animals are divided by color-code. In each graph, the R and the p – value of the linear regression are reported. Figure Contributions: AC, RA, EMR and ES performed the experiments and collected the data. AC analyzed the data.

References

- Beaud, M. L. *et al.* (2008) 'Anti-Nogo-A antibody treatment does not prevent cell body shrinkage in the motor cortex in adult monkeys subjected to unilateral cervical cord lesion', *BMC Neuroscience*. doi: 10.1186/1471-2202-9-5.
- Beaud, M. L. *et al.* (2012) 'Invasion of lesion territory by regenerating fibers after spinal cord injury in adult macaque monkeys', *Neuroscience*. doi: 10.1016/j.neuroscience.2012.09.052.
- Boudrias, M. H. *et al.* (2010) 'Forelimb muscle representations and output properties of motor areas in the mesial wall of rhesus macaques', *Cerebral Cortex*. doi: 10.1093/cercor/bhp136.
- Carrera, E. and Tononi, G. (2014) 'Diaschisis: Past, present, future', *Brain*. doi: 10.1093/brain/awu101.
- Chao, Z. C. *et al.* (2019) 'Dynamic Reorganization of Motor Networks During Recovery from Partial Spinal Cord Injury in Monkeys', *Cerebral Cortex*. doi: 10.1093/cercor/bhy172.
- Contestabile, A. *et al.* (2018) 'Asymmetric and Distant Effects of a Unilateral Lesion of the Primary Motor Cortex on the Bilateral Supplementary Motor Areas in Adult Macaque Monkeys', *The Journal of Neuroscience*. doi: 10.1523/jneurosci.0904-18.2018.
- Courtine, G. *et al.* (2007) 'Stance- and Locomotion-Dependent Processing of Vibration-Induced Proprioceptive Inflow From Multiple Muscles in Humans', *Journal of Neurophysiology*. doi: 10.1152/jn.00764.2006.
- Dancause, N. *et al.* (2005) 'Extensive cortical rewiring after brain injury.', *The Journal of neuroscience : the official journal of the Society for Neuroscience*. doi: 10.1523/JNEUROSCI.3256-05.2005.
- Dum, R. P. and Strick, P. L. (1996) 'Spinal cord terminations of the medial wall motor areas in macaque monkeys.', *The Journal of neuroscience : the official journal of the Society for Neuroscience*.
- Finger, S., Koehler, P. J. and Jagella, C. (2004) 'The Monakow Concept of Diaschisis: Origins and Perspectives', *Archives of Neurology*. doi: 10.1001/archneur.61.2.283.
- Fregosi, M. *et al.* (2017) 'Corticobulbar projections from distinct motor cortical areas to the reticular formation in macaque monkeys', *European Journal of Neuroscience*. doi:

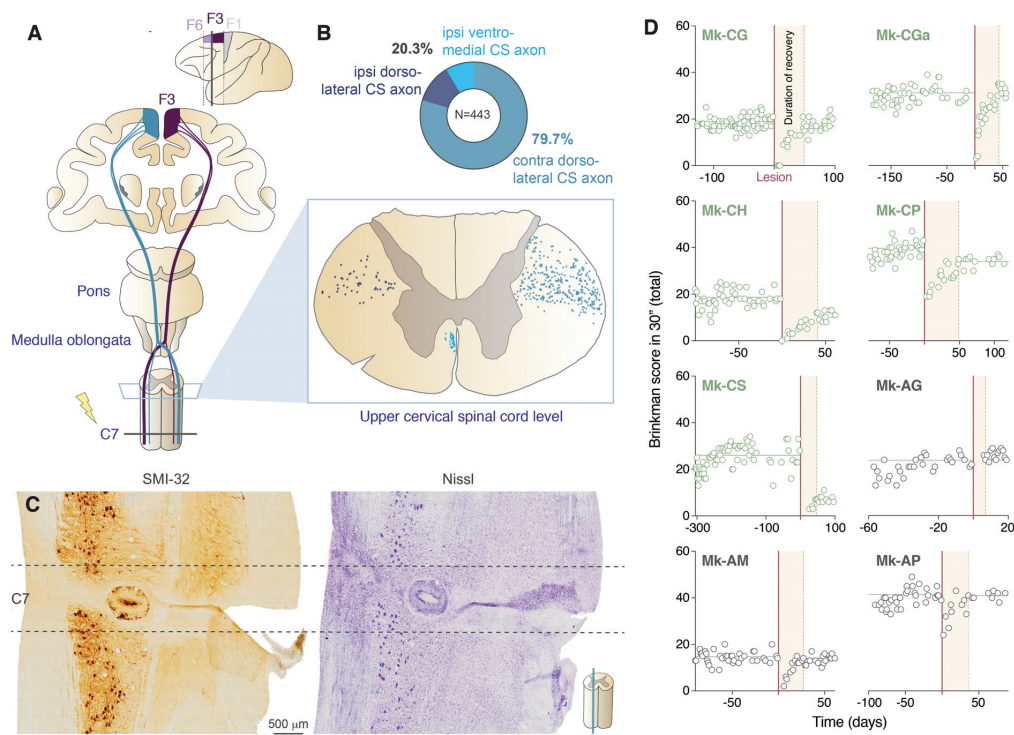
- 699 10.1111/ejn.13576.
- 700 Fregosi, M. *et al.* (2018) 'Changes of motor corticobulbar projections following different lesion
- 701 types affecting the central nervous system in adult macaque monkeys', *European Journal of*
- 702 *Neuroscience*. doi: 10.1111/ejn.14074.
- 703 Fregosi, M. and Rouiller, E. M. (2017) 'Ipsilateral corticotectal projections from the primary,
- 704 premotor and supplementary motor cortical areas in adult macaque monkeys: a quantitative
- 705 anterograde tracing study', *European Journal of Neuroscience*. doi: 10.1111/ejn.13709.
- 706 Freund, P. *et al.* (2006) 'Nogo-A-specific antibody treatment enhances sprouting and
- 707 functional recovery after cervical lesion in adult primates', *Nature Medicine*. doi:
- 708 10.1038/nm1436.
- 709 Freund, P. *et al.* (2007) 'Anti-Nogo-A antibody treatment enhances sprouting of corticospinal
- 710 axons rostral to a unilateral cervical spinal cord lesion in adult macaque monkey', *Journal of*
- 711 *Comparative Neurology*. doi: 10.1002/cne.21321.
- 712 Freund, P. *et al.* (2009) 'Anti-Nogo-A antibody treatment promotes recovery of manual
- 713 dexterity after unilateral cervical lesion in adult primates - Re-examination and extension of
- 714 behavioral data', *European Journal of Neuroscience*. doi: 10.1111/j.1460-
- 715 9568.2009.06642.x.
- 716 Galea, M. P. and Darian-Smith, I. (1997) 'Manual dexterity and corticospinal connectivity
- 717 following unilateral section of the cervical spinal cord in the macaque monkey', *Journal of*
- 718 *Comparative Neurology*. doi: 10.1002/(SICI)1096-9861(19970512)381:3<307::AID-
- 719 CNE4>3.0.CO;2-6.
- 720 Genç, B. *et al.* (2017) 'Apical dendrite degeneration, a novel cellular pathology for Betz cells
- 721 in ALS', *Scientific Reports*. doi: 10.1038/srep41765.
- 722 Geyer, S. *et al.* (2000) 'Neurofilament protein distribution in the macaque monkey
- 723 dorsolateral premotor cortex', *European Journal of Neuroscience*. doi: 10.1046/j.1460-
- 724 9568.2000.00042.x.
- 725 Ghosh, A. *et al.* (2009) 'Functional and anatomical reorganization of the sensory-motor
- 726 cortex after incomplete spinal cord injury in adult rats', *Journal of Neuroscience*. doi:

- 10.1523/JNEUROSCI.1828-09.2009.
- Hashimoto, M. *et al.* (2004) 'Regulation of semaphorin 3A expression in neurons of the rat spinal cord and cerebral cortex after transection injury', *Acta Neuropathologica*. doi: 10.1007/s00401-003-0805-z.
- Hoogewoud, F. *et al.* (2013) 'Comparison of functional recovery of manual dexterity after unilateral spinal cord lesion or motor cortex lesion in adult macaque monkeys', *Frontiers in Neurology*. doi: 10.3389/fneur.2013.00101.
- Isa, T. and Nishimura, Y. (2014) 'Plasticity for recovery after partial spinal cord injury - Hierarchical organization', *Neuroscience Research*. doi: 10.1016/j.neures.2013.10.008.
- Jenny, A. B., Inukai, J. and Strick, P. (1983) 'Principles of motor organization of the monkey cervical spinal cord.', *The Journal of neuroscience : the official journal of the Society for Neuroscience*.
- Kaesler, M. *et al.* (2011) 'Autologous adult cortical cell transplantation enhances functional recovery following unilateral lesion of motor cortex in primates: A pilot study', *Neurosurgery*. doi: 10.1227/NEU.0b013e31820c02c0.
- Kaesler, M. *et al.* (2014) 'Variability of manual dexterity performance in non-human primates (Macaca fascicularis)', *International Journal of Comparative Psychology*, 27(2).
- Lawrence, D. G. and Kuypers, H. G. J. M. (1968) 'The functional organization of the motor system in the monkey: I. The effects of bilateral pyramidal lesions', *Brain*. doi: 10.1093/brain/91.1.1.
- Lemon, R. N. (2008) 'Descending Pathways in Motor Control', *Annual Review of Neuroscience*. doi: 10.1146/annurev.neuro.31.060407.125547.
- Liu, J. *et al.* (2002) 'Origins of callosal projections to the supplementary motor area (SMA): A direct comparison between pre-SMA and SMA-proper in macaque monkeys', *Journal of Comparative Neurology*. doi: 10.1002/cne.10087.
- Liu, Y. and Rouiller, E. M. (1999) 'Mechanisms of recovery of dexterity following unilateral lesion of the sensorimotor cortex in adult monkeys', in *Experimental Brain Research*. doi: 10.1007/s002210050830.

- 755 Lundell, H. *et al.* (2011) 'Cerebral activation is correlated to regional atrophy of the spinal
756 cord and functional motor disability in spinal cord injured individuals', *NeuroImage*. doi:
757 10.1016/j.neuroimage.2010.09.009.
- 758 Luppino, G. *et al.* (1994) 'Corticospinal projections from mesial frontal and cingulate areas in
759 the monkey', *NeuroReport*. doi: 10.1097/00001756-199412000-00035.
- 760 Maier, M. A. *et al.* (2002) 'Differences in the corticospinal projection from primary motor
761 cortex and supplementary motor area to macaque upper limb motoneurons: an anatomical
762 and electrophysiological study.', *Cerebral cortex (New York, N.Y. : 1991)*. doi:
763 10.1093/cercor/12.3.281.
- 764 McNeal, D. W. *et al.* (2010) 'Selective long-term reorganization of the corticospinal projection
765 from the supplementary motor cortex following recovery from lateral motor cortex injury',
766 *Journal of Comparative Neurology*. doi: 10.1002/cne.22218.
- 767 von Monakow, C. (1914) 'Die Lokalisation im Grosshirn und der Abbau der Funktion durch
768 Kortikale Herde.', *Journal of the American Medical Association*. doi:
769 10.1001/jama.1914.02570090083033.
- 770 Morecraft, R. J. *et al.* (2015) 'Vulnerability of the medial frontal corticospinal projection
771 accompanies combined lateral frontal and parietal cortex injury in rhesus monkey', *Journal of*
772 *Comparative Neurology*. doi: 10.1002/cne.23703.
- 773 Morecraft, R. J. *et al.* (2016) 'Frontal and frontoparietal injury differentially affect the
774 ipsilateral corticospinal projection from the nonlesioned hemisphere in monkey (*Macaca*
775 *mulatta*)', *Journal of Comparative Neurology*. doi: 10.1002/cne.23861.
- 776 Nevian, T. *et al.* (2007) 'Properties of basal dendrites of layer 5 pyramidal neurons: A direct
777 patch-clamp recording study', *Nature Neuroscience*. doi: 10.1038/nn1826.
- 778 Nishimura, Y. *et al.* (2007) 'Time-dependent central compensatory mechanisms of finger
779 dexterity after spinal cord injury', *Science*. doi: 10.1126/science.1147243.
- 780 Nishimura, Y. and Isa, T. (2009) 'Compensatory changes at the cerebral cortical level after
781 spinal cord injury', *Neuroscientist*. doi: 10.1177/1073858408331375.
- 782 Nishimura, Y. and Isa, T. (2012) 'Cortical and subcortical compensatory mechanisms after

- 783 spinal cord injury in monkeys', *Experimental Neurology*. doi:
 784 10.1016/j.expneurol.2011.08.013.
- 785 Orczykowski, M. E. *et al.* (2018) 'Cell based therapy enhances activation of ventral premotor
 786 cortex to improve recovery following primary motor cortex injury', *Experimental Neurology*.
 787 doi: 10.1016/j.expneurol.2018.03.010.
- 788 Rathelot, J.-A. and Strick, P. L. (2009) 'Subdivisions of primary motor cortex based on
 789 cortico-motoneuronal cells', *Proceedings of the National Academy of Sciences*. doi:
 790 10.1073/pnas.0808362106.
- 791 Rouiller, E. M. *et al.* (1994) 'Transcallosal connections of the distal forelimb representations
 792 of the primary and supplementary motor cortical areas in macaque monkeys', *Experimental*
 793 *Brain Research*. doi: 10.1007/BF00227511.
- 794 Rouiller, E. M. (1996) 'Evidence for direct connections between the hand region of the
 795 supplementary motor area and cervical motoneurons in the Macaque monkey', *European*
 796 *Journal of Neuroscience*. doi: 10.1111/j.1460-9568.1996.tb01592.x.
- 797 Savidan, J. *et al.* (2017) 'Role of primary motor cortex in the control of manual dexterity
 798 assessed via sequential bilateral lesion in the adult macaque monkey: A case study',
 799 *Neuroscience*. doi: 10.1016/j.neuroscience.2017.06.018.
- 800 Schmidlin, E. *et al.* (2011) 'Behavioral Assessment of Manual Dexterity in Non-Human
 801 Primates', *Journal of Visualized Experiments*. doi: 10.3791/3258.
- 802 Sternberger, L. A. and Sternberger, N. H. (1983) 'Monoclonal antibodies distinguish
 803 phosphorylated and nonphosphorylated forms of neurofilaments in situ.', *Proceedings of the*
 804 *National Academy of Sciences of the United States of America*.
- 805 Sugiyama, Y. *et al.* (2013) 'Effects of early versus late rehabilitative training on manual
 806 dexterity after corticospinal tract lesion in macaque monkeys', *Journal of Neurophysiology*.
 807 doi: 10.1152/jn.00814.2012.
- 808 Urrego, D., Troncoso, J. and Múnera, A. (2015) 'Layer 5 Pyramidal Neurons' Dendritic
 809 Remodeling and Increased Microglial Density in Primary Motor Cortex in a Murine Model of
 810 Facial Paralysis', *BioMed Research International*. doi: 10.1155/2015/482023.

- 811 Wang, W. *et al.* (2019) 'Reorganization of the brain in spinal cord injury: a meta-analysis of
812 functional MRI studies', *Neuroradiology*. doi: 10.1007/s00234-019-02272-3.
- 813 Wannier, T. *et al.* (2005) 'A Unilateral Section of the Corticospinal Tract at Cervical Level in
814 Primate Does Not Lead to Measurable Cell Loss in Motor Cortex', *Journal of Neurotrauma*.
815 doi: 10.1089/neu.2005.22.703.
- 816 De Winter, F. *et al.* (2002) 'Injury-induced class 3 semaphorin expression in the rat spinal
817 cord', *Experimental Neurology*. doi: 10.1006/exnr.2002.7884.
- 818 Yoshida, Y. and Isa, T. (2018) 'Neural and genetic basis of dexterous hand movements',
819 *Current Opinion in Neurobiology*. doi: 10.1016/j.conb.2018.04.005.
- 820 Zaaïmi, B. *et al.* (2012) 'Changes in descending motor pathway connectivity after
821 corticospinal tract lesion in macaque monkey', *Brain*. doi: 10.1093/brain/aws115.
- 822 Zhou, W. L. *et al.* (2008) 'Dynamics of action potential backpropagation in basal dendrites of
823 prefrontal cortical pyramidal neurons', *European Journal of Neuroscience*. doi:
824 10.1111/j.1460-9568.2008.06075.x.
- 825



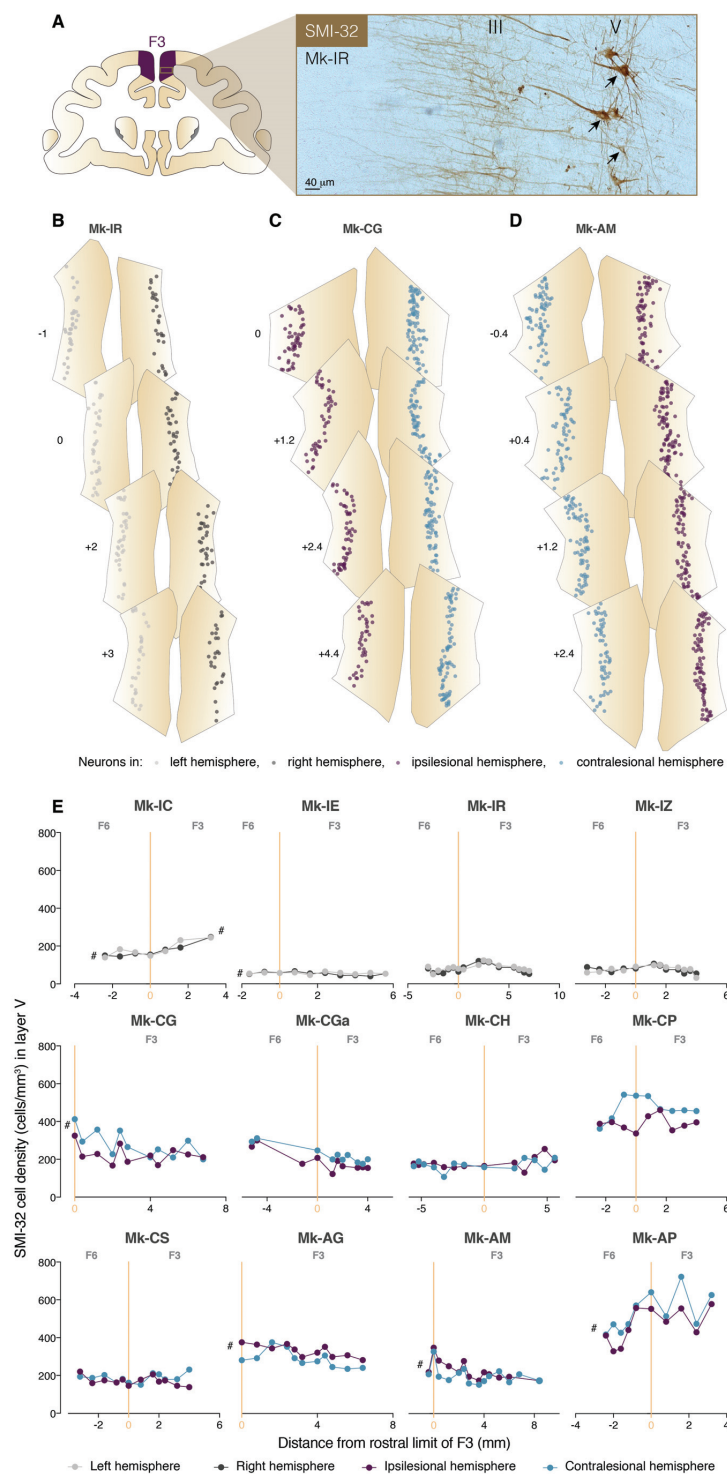


Figure 2 - Contestabile et al

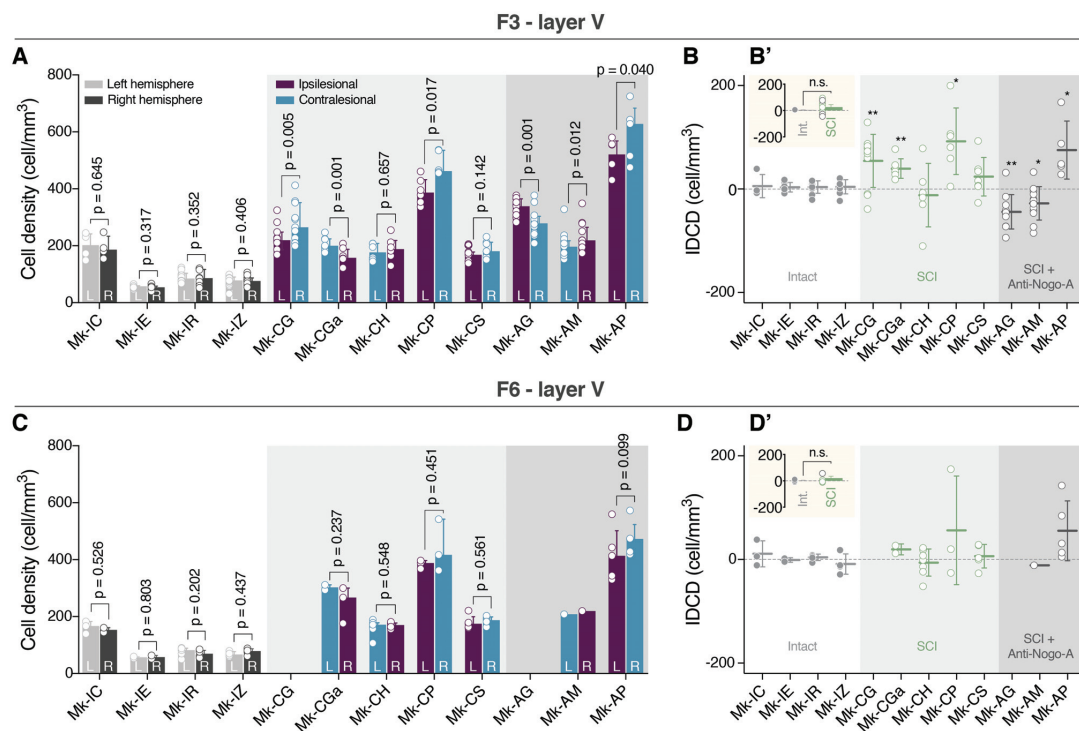


Figure 3 - Contestabile et al

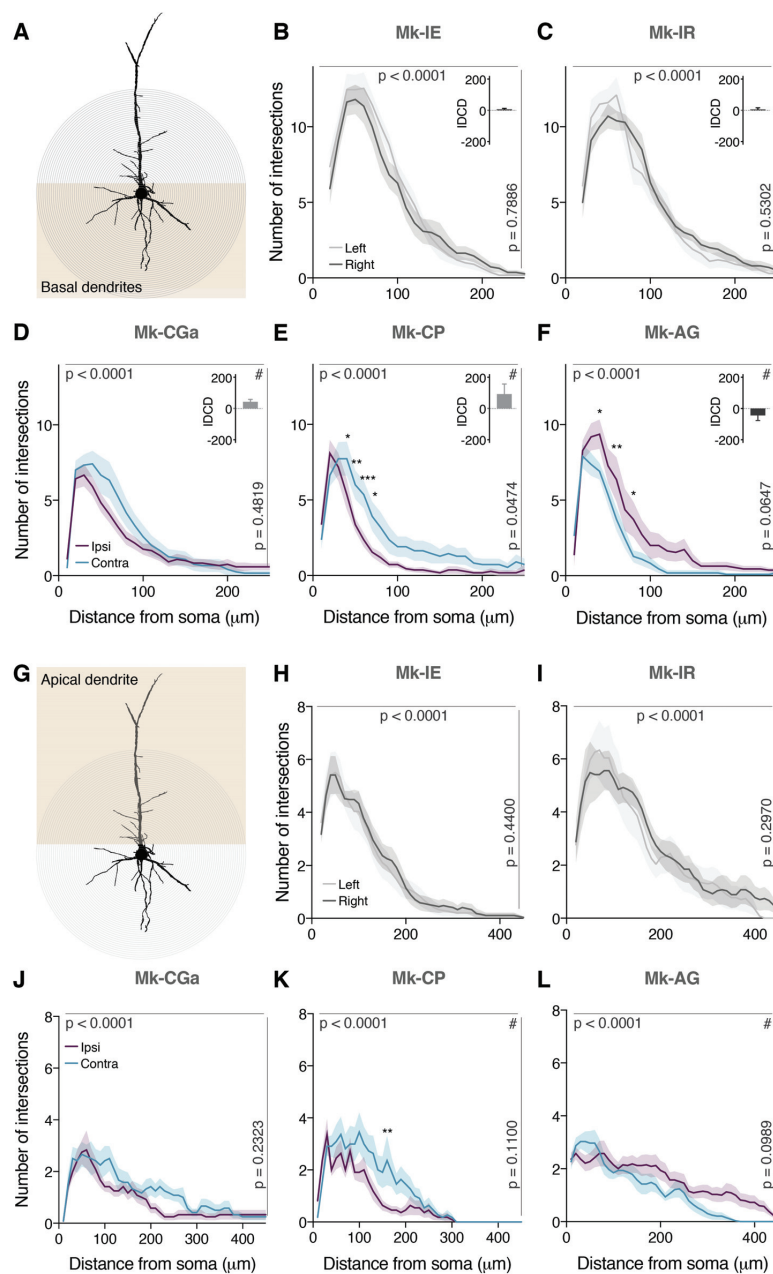


Figure 4 - Contestabile et al

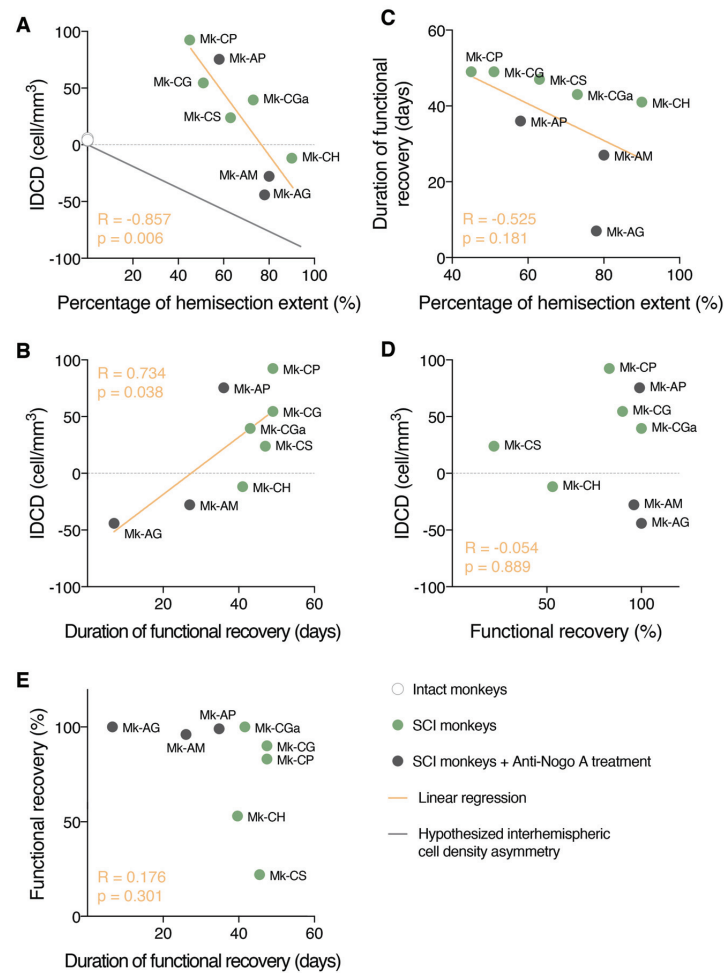


Figure 5 - Contestabile et al